Astronomy
&
Astrophysics

Discovery of a high-redshift Einstein ring[⋆]

R. A. Cabanac[1,2,3], D. Valls-Gabaud[3,4], A. O. Jaunsen[2], C. Lidman[2], and H. Jerjen[5]

[1] Dep. de Astronomía y Astrofísica, Pontificia Universidad Católica de Chile, Casilla 306, Santiago, Chile
    e-mail: cabanac@cfht.hawaii.edu
[2] European Southern Observatory, Alonso de Cordova 3107, Casilla 19001, Santiago, Chile
[3] Canada-France-Hawaii Telescope, 65-1238 Mamalahoa Highway, Kamuela, HI 96743, USA
[4] CNRS UMR 5572, LATT, Observatoire Midi-Pyrénées, 14 Av. E. Belin, 31400 Toulouse, France
[5] Research School of Astronomy and Astrophysics, ANU, Mt. Stromlo Observatory, Weston ACT 2611, Australia

Received 24 December 2004 / Accepted 26 April 2005

Abstract. We report the discovery of a partial Einstein ring of radius $1''.48$ produced by a massive (and seemingly isolated) elliptical galaxy. The spectroscopic follow-up at the VLT reveals a $2L_\star$ galaxy at $z = 0.986$, which is lensing a post-starburst galaxy at $z = 3.773$. This unique configuration yields a very precise measure of the mass of the lens within the Einstein radius, $(8.3 \pm 0.4) \times 10^{11} h_{70}^{-1}\ M_\odot$. The fundamental plane relation indicates an evolution rate of $\mathrm{dlog}(M/L)_B/\mathrm{d}z = -0.57 \pm 0.04$, similar to other massive ellipticals at this redshift. The source galaxy shows strong interstellar absorption lines indicative of large gas-phase metallicities, with fading stellar populations after a burst. Higher resolution spectra and imaging will allow the detailed study of an unbiased representative of the galaxy population when the universe was just 12% of its current age.

Key words. cosmology: observations – gravitational lensing – galaxies: high-redshift – ellipticals –
evolution – FOR J0332-3557

1. Introduction

One of the key issues in galaxy formation within the current ΛCDM framework of structure formation is the mass assembly histories of galactic halos. In this paradigm, the growth of halo mass through mergers produces giant galaxies and star formation appears rather late during this process. Measuring the evolution of the mass-to-light ratio hence constrains directly this formation scenario, and provides clues on the evolution of the fundamental plane. Various deep surveys have uncovered different galaxy populations, but the selection criteria produce biased samples: UV-selected (Steidel et al. 2003) and narrow-band selected (Hu et al. 2002) samples are sensitive to actively star-forming galaxies and biased against quiescent, evolved systems, while sub-millimeter (Blain et al. 2000) and near-infrared surveys (McCarthy et al. 2001; Abraham et al. 2004) select dusty starburst galaxies and very red galaxies respectively. It is not clear how representative these samples are of the population of distant galaxies as a whole and how they are related to present-day galaxies. In contrast, selection through gravitational lensing is not biased, as any distant galaxy which happens to have a massive deflector along the line of sight can be amplified. This technique has yielded many examples of very distant galaxies, amplified by the mass distribution of

foreground clusters of galaxies. (Ellis et al. 2001; Pettini et al. 2002; Pelló et al. 2004). Configurations where lenses are isolated and distant ($z \sim 1$) galaxies are much rarer and yet provide direct measures of the total mass without any assumptions on stellar evolution. Whilst the total mass enclosed within the projected Einstein radius θ_E can be well measured with systems presenting a few ($\sim$2–4) images of the lensed galaxy, many more constraints are given by the observations of nearly-complete Einstein rings (Kochanek et al. 2001), as they do not suffer from the well-known ellipticity-shear degeneracy due to the many data along different position angles.

Although many arcs have been discovered, associated with massive galaxy clusters and their dominant central galaxies, there are very few optical rings (Miralda-Escudé & Léhar 1992) or arcs, especially at high redshifts. Only a few systems with lenses above $z_l \sim 0.9$ are known: CFRS 03.1077 ($z_l = 0.938, z_s = 2.941$, Crampton et al. 2002), MG 0414+0534 ($z_l = 0.958, z_s = 2.62$, Hewitt et al. 1992; Tonry & Kochanek 1999), MG 2016+112 ($z_l = 1.004, z_s = 3.273$, Lawrence et al. 1984; Koopmans & Treu 2002), and possibly J100424.9+122922 ($z_l \sim 0.95, z_s = 2.65$, Lacy et al. 2002) and GDS J033206−274729 ($z_l \sim 0.96$, Fassnacht et al. 2004). In all cases the arcs cover less than 60 degrees around the central lens and hence are not nearly-complete Einstein rings. The only optical ring reported so far (Warren et al. 1996), over some 170° with a radius $1''.08$, is a galaxy at $z_s = 3.595$ lensed by an elliptical galaxy at a much smaller $z_l = 0.485$.

Here we report the discovery of a fourth confirmed system, dubbed FOR J0332−3557 ($03^{\rm h}32^{\rm m}59\overset{\rm s}{.}94$, $-35°57'51\overset{''}{.}7$, J2000), in a sight line through the outskirts of the Fornax cluster, where the reddening of our Galaxy is $E(B-V) = 0.02$ (Schlegel et al. 1998). This new system is remarkable on two accounts. First, it is a bright, almost complete Einstein ring of radius $1\overset{''}{.}48$, covering some 260° around the lens, extending over $4'' \times 3''$ (Sect. 2) and with a total apparent magnitude $R_{\rm c} = 22.2$. As discussed in Sect. 3, the lens appears to be an elliptical galaxy at $z_{\rm l} = 0.986$. Second, the lensed source is a galaxy at redshift $z_{\rm s} = 3.773$ (Sect. 4). A flat FRW metric with $\Omega_{\rm m} = 0.3$, $\Omega_\Lambda = 0.7$ and $H_0 = 70 \, h_{70}$ km s^{-1} Mpc^{-1} is assumed.

2. Modeling the gravitational lensing system

Full details of the observational photometric and spectroscopic setups will be reported elsewhere (Cabanac et al. 2005). Given the excellent image quality in the $R_{\rm c}$ band, with $0\overset{''}{.}5$ seeing, a detailed modeling of the lensing system can be carried out. We followed the procedure pioneered by Kochanek et al. (2001) with two important differences. First, not only we use the detailed shape of the ring (ridge) and the flux along the ridge, but also the width of the ring along each radial direction. These three sets of observables were incorporated into a likelihood function. Second, since we do not want to impose any a priori information, the problem has a high dimensionality: 5 parameters to describe the properties of the lens (given a mass profile: the normalisation, ellipticity and orientation, plus an external shear and its orientation) and 5 for the source (position with respect to the lens, effective radius, ellipticity and orientation). Hence, to guarantee that the maximum likelihood of the fit was found in the 10-dimensional parameter space, we coupled a state-of-the-art genetic algorithm developed by one of us with the `gravlens` code (Keeton 2001). Briefly stated, the parameters are coded in the chromosome of an individual which can produce two offsprings from its coupling with another individual (Charbonneau 1995). For each individual in each generation (i.e. one configuration in parameter space), we compute the resulting image, convolve it with the seeing of the VLT image, and measure its likelihood. These steps are illustrated in Fig. 1. After a few thousand generations the genetic algorithm finds the absolute maximum of the likelihood, and several tests were made to assess that different runs always converged to the same solution. From the ensemble of generations and individuals the likelihood contours can be computed and the partial correlations and degeneracies between parameters explored. The procedure will be presented in detail elsewhere.

Following Kassiola & Kovner (1993); Kormann et al. (1994); Keeton et al. (1998), projected surface mass density for an isothermal ellipsoid (SIE) written in polar coordinates (r, ϕ) and expressed in units of the critical density for lensing is

$$\kappa(r, \phi) = \frac{b}{2r}\left[\frac{1+q^2}{(1+q^2)-(1-q^2)\cos 2\phi}\right],$$

where $q \leq 1$ is the axial ratio. The radius r and the parameter b both have dimensions of length (expressed here in arcsec). b is
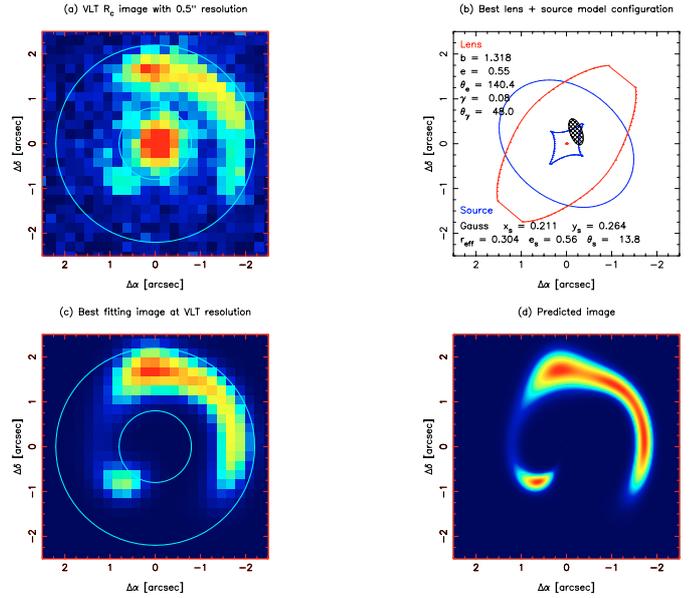

Fig. 1. a) Image of the ring with $0\overset{''}{.}5$ seeing, **b)** best configuration for the lens and the source, with the position of the caustics (cf. text for parameter definitions), **c)** best-fitting image convolved with the seeing, and **d)** the predicted image at the resolution of HST/ACS.

equal to the Einstein radius $\theta_{\rm E}$ in the spherical case. Following Huterer et al. (2004) we use an Einstein radius

$$\theta_{\rm E} = b \exp[(0.89e)^3],$$

for a non-spherical SIE of ellipticity $e = 1 - q$.

Figure 1 shows the best-fit case with $b = 1\overset{''}{.}318 \pm 0.02$ and $e = 0.55 \pm 0.01$, yielding $\theta_{\rm E} = 1\overset{''}{.}48 \pm 0\overset{''}{.}02$, that is, 11.8 h_{70}^{-1} kpc, with possibly a systematic error of 9% due to the different possible normalisations of isothermal ellipsoids (Huterer et al. 2004). Given the redshifts of the lens (Sect. 3) and the source (Sect. 4), the total mass within the Einstein radius is $M_{\rm E} = (8.3 \pm 0.2) \times 10^{11} \, h_{70}^{-1} \, M_\odot$. The lens is 20% less massive than the elliptical lens in MG 2016+112 at $z_{\rm l} = 1.004$ (Koopmans & Treu 2002). Quite independently of the assumed elliptical potential, the derived magnification of the source is 12.9. The mass ellipticity appears to be larger than the light ellipticity of 0.2 (Sect. 3) but this is often found in other systems (Keeton et al. 1998).

The large number of constraints provided by the ring lifts the degeneracy between the flattening of the potential and the external shear. For a wide range of potentials we consistently find high flattenings and small shears. The small value of the shear (Fig. 1b) $\gamma = 0.08 \pm 0.01$ is typical of those found in loose groups of galaxies. Given its direction (48°) it is possible that the shear is caused by a faint nearby galaxy which lies $\zeta = 5\overset{''}{.}7$ away at a position angle $38° \pm 0\overset{\circ}{.}5$ and with a photometric redshift of ~1.27. If this is the case, the galaxy would have a SIS Einstein radius of $\theta_{\rm E} = 2\gamma\zeta = 0\overset{''}{.}91$ and a projected velocity dispersion of 260 km s^{-1}. It would imply a massive galaxy, inconsistent with its observed brightness. On the other hand, the $R_{\rm c}$ and B images show a diffuse population of blue galaxies within one arcmin of the Einstein ring, and the near-IR images in J, H, and $K_{\rm s}$ provide evidence for a group of galaxies
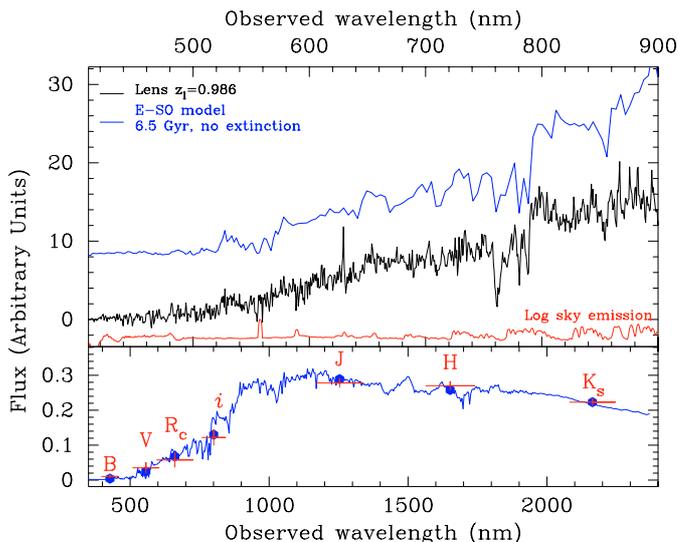
Fig. 2. *Top*: the spectrum of the lens (middle black line), the underlying sky emission (bottom red line), and the HYPERZ-derived best-fit synthetic spectrum (top blue line). *Bottom*: observed BVR_ciJHK_s photometry and the spectral energy distribution of the best-fitting spectrum shown above.

possibly associated with the lens or else with a proto-cluster at redshift 2 as the photometric redshifts with HYPERZ (Bolzonella et al. 2000) show a bimodal probability distribution function with peaks at both redshifts. There is no evidence, however, for a red sequence at $z \approx 1$.

3. The lens galaxy

The BVR_ciJHK_s multicolour images obtained at ESO/VLT/La Silla and the optical spectrum of the lens (Fig. 2) constrain the spectral energy distribution (SED) unambiguously and allow the precise identification of the lens as a quiescent galaxy at redshift $z_l = 0.986 \pm 0.005$.

We used GALFIT (Peng et al. 2002) to fit the profile of the lens, using a PSF-corrected profile with de Vaucouleurs, Sersic and exponential parameterizations, masking the ring and using a range of sky level (average $\pm 3\sigma$). This yields best-fit de Vaucouleurs[1] profiles with effective radii and average surface brightnesses given Table 1, and consistently small ellipticities $e = 1-q = 0.20 \pm 0.1$ in all bands. This distant lens appears rounder than the nearby ones, where the mean observed light ellipticity is 0.31 ± 0.18 (Jorgensen et al. 1995).

The fitted SED (Fig. 2) allows one to infer properly the k corrections following Poggianti (1997): we find $B_{rest} - R_{cobs} = -0.65$, $B_{rest} - i_{obs} = 0.73$ and $B_{rest} - J_{obs} = 3.08$, yielding a consistent $B_{rest} = 21.7 \pm 0.1$. Using other templates which provide similar good fits to the SED yield the same result. For sake of completeness, it should be noted that HYPERZ can also fit (with a lower probability) bluer templates of *younger* ages with extinctions of up to $A_V = 0.8$ mag, assuming a Seaton extinction

---

[1] Sersic profiles also fit the surface brightness with values of $n > 3$, the dominant parameter in the Chi-square fit is the background subtraction, but since we find no hint of a disk in the R band (blue rest-frame), we used a de Vaucouleurs' profile parameterization.

Table 1. Photometric properties of the lens galaxy.

Band	Effective radius R_e		$\langle \mu \rangle^1$	m_{tot}
	['']	[h_{70}^{-1} kpc]	[mag arcsec^{-2}]	[mag]
R_c	0.36 ± 0.05	2.9 ± 0.4	22.20 ± 0.10	22.42
i	0.36	2.9	20.70 ± 0.20	20.92
J	0.41 ± 0.01	3.3 ± 0.1	18.64 ± 0.03	18.58
H	0.43 ± 0.01	3.4 ± 0.1	17.70 ± 0.03	17.54
K_s	0.50 ± 0.01	4.0 ± 0.1	17.13 ± 0.03	16.63

[1] $\langle \mu \rangle$ is the average surface brightness, not to be confused with the surface brightness at the effective radius $\mu(R_e) = \mu_e$.

law (1979). The definitive internal extinction of the lens can only be better constrained with a higher quality spectrum of higher resolution.

If we assume that the lens is an elliptical galaxy, we can compare its measured optical properties with the nearby and high-redshift sample. The rest-frame $M_B = -22.3$ is twice brighter than the typical galaxies at $z \sim 1$ which have $M_B^\star = -21.5 \pm 0.2$, and its rest-frame $U - V$ colour is redder (1.31) than the average $L_\star$ galaxy at this redshift ($U - V = 1.10 \pm 0.1$, Bell et al. 2004), while its rest-frame $U - B = 0.18$ appears bluer than similar field ellipticals (Gebhardt et al. 2003).

The rest-frame absolute B-band surface brightness SB$_B$, inferred from the R_c (resp. J) images, yield SB$_B$ = 18.57 $\pm$ 0.10 (18.75) mag arcsec^{-2} after the $(1 + z)^4$ cosmological corrections. The fundamental plane relation of elliptical galaxies can be written as

$$\Gamma_i = \log(R_e/\text{kpc}) - \alpha \log \sigma - \beta \, \text{SB}_B,$$

where R_e is the effective radius, σ is the velocity dispersion, and we adopt $\alpha = 1.25$, $\beta = 0.32$ and $\Gamma_0 = -9.04 - \log h_{70}$ (Treu & Koopmans 2004). Taking the velocity dispersion inferred from the lens modeling (Sect. 2) as $\sigma = 302 \pm 12$(syst) km s^{-1}, the evolution in the mass to light ratio becomes

$$\Delta \log(M/L_B) = -(\Gamma_i - \Gamma_0)/2.5\beta = -0.57 \pm 0.04$$

where the uncertainty takes into account the systematics in the dispersion velocity and the effective radius. This evolution rate is consistent with what is observed in field or cluster ellipticals (Gebhardt et al. 2003; Rusin et al. 2003; Koopmans & Treu 2003), and within the scatter seen for massive galaxies (Treu et al. 2005) at these redshifts. It also implies a relatively large formation redshift, in a simplified scenario where star formation proceeds in a single burst. This is consistent with the SED-inferred stellar population. We note that the radio ring MG 1131+0456 (whose lens is at $z_l = 0.844$, Tonry & Kochanek 2000) also yields a smaller evolutionary rate (Rusin et al. 2003).

Assuming that the evolution of the stellar mass-to-light ratio is the same as the effective one derived above, and taking a value of 7.8 ± 2.2 h_{70} $M_\odot/L_{B\odot}$ for the local galaxies, results in $(M_*/L_B) = 2.1 \pm 0.1$ h_{70} $M_\odot/L_{B\odot}$, entirely consistent with relatively old stellar populations (as corroborated by the best fitting SED, Fig. 2). However, at the Einstein radius θ_E the ratio $M(< \theta_E)/L_B(< \theta_E) = 7.1 \pm 0.5$ h_{70} $M_\odot/L_{B\odot}$.
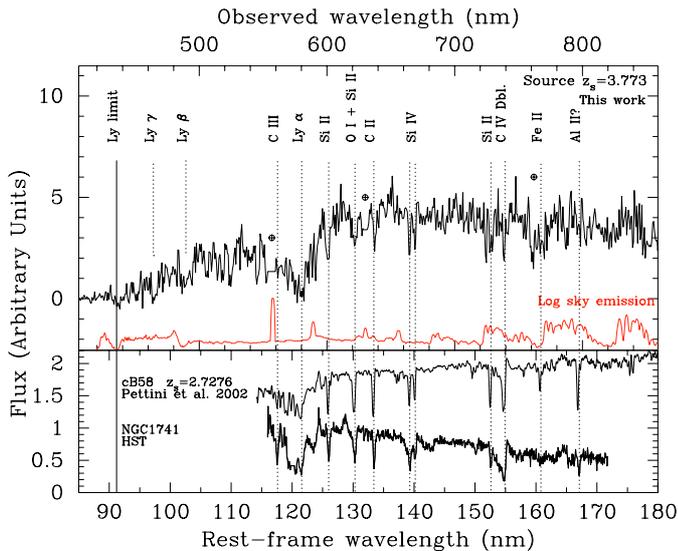
Fig. 3. *Top*: the spectrum of the source galaxy, showing strong lines from the interstellar medium, yields a redshift of 3.773 ± 0.003. *Bottom*: the shape of the continuum and the depth of the lines are consistent with a population of stars having past a major episode of star formation, very similar to the post-starburst galaxies shown in comparison, both distant (cB58) or nearby (NGC 1741). The sky emission and some telluric lines are also indicated.

4. The source galaxy

The VLT/FORS low-resolution spectrum of the lensed source (Fig. 3) reveals a galaxy at a redshift $z_s = 3.773 \pm 0.003$. Its apparent total magnitude $R_c = 22.6$ makes it about one magnitude brighter than the brightest Lyman-break galaxies (LBGs) found at $z \sim 3.5$ (Steidel et al. 2003). The source is sufficiently bright to make future follow-up kinematic and abundance studies of its interstellar medium similar to what was possible on the $z_s = 2.73$ lensed galaxy cB58 (Pettini et al. 2002).

The overall spectrum compares well with the high luminosity Lyman-break galaxies (Shapley et al. 2003) which have Lyα in absorption at $z \sim 3$ or even with SDSS J1147−0250 (Bentz et al. 2004) at a lower redshift. The continuum appears to be rather flat, bluer than cB58 but redder than NGC 1741, and it is remarkable that there are no emission lines (with the possible exception of C III] $\lambda\lambda$ 190.7,190.9). It is clearly not like the H II galaxy detected at a similar redshift ($z = 3.357$) in the Lynx arc (Fosbury et al. 2003). The flat continuum and the absence of Lyα in emission, as seen in many nearby starbursts and about half the LBGs, is consistent with a post-burst stellar population, where the absorption stellar Lyα line becomes important after a few million years (Valls-Gabaud 1993) independently of metallicity or extinction.

Although the resolution of the discovery spectrum is not high enough to make a kinematic study of the different lines, the signal-to-noise is sufficient to allow the identification of many photospheric and interstellar medium absorption features with the following rest-frame equivalent widths (in nm): C II $\lambda133.5$ (0.15 ± 0.02), C IV $\lambda\lambda154.8,155.1$ (0.08 ± 0.02), O I/Si II [blend]$\lambda\lambda$ 130.2,130.4 (0.17 ± 0.02), Si II $\lambda126.0$ (0.30 ± 0.04), Si II $\lambda152.7$ (0.25 ± 0.04), Si IV $\lambda139.4$ (0.13 ± 0.02), Si IV $\lambda140.3$ (0.08 ± 0.02). There

are also tentative detections of other important lines, such as Fe II $\lambda160.8$, C III $\lambda117.6$, and Al II $\lambda167.0$, along with possible features produced by P V and O I. The metallicity index at 143.5 nm is contaminated by sky lines, but the pattern that emerges from these values, although preliminary, is that the gas-phase abundances of these interstellar absorption lines are rather high, especially in comparison with cB58 (Pettini et al. 2002). In this respect, the source galaxy appears more similar to the LBGs at $z \sim 5$ (Ando et al. 2004) where the ISM lines are stronger than at $z = 3$ (with the notable exception of carbon). These indications point to a very rapid enrichment by type II supernovae, associated to bursts of star formation, in many respects similar to the pattern seen in star-forming galaxies at $z \sim 2.2$ (Shapley et al 2004).

The flux at 150 nm has been traditionally used to measure the star formation rate from UV spectra. Calibrating on the well-measured R_c magnitude, we derive a flux density at 150 nm of 2.15μJy (assuming a conversion factor of 2875 Jy for a $R_c = 0$ source), which translates into $SFR_{UV} \approx 31 \, (A/12.9)^{-1} \, h_{70}^{-2} \, M_\odot \, \text{a}^{-1}$, adopting the standard relation (Kennicutt 1998, and where A is the gravitational amplification produced by the lens (Sect. 2)). There are two important caveats. First, this could be a lower value because we have neglected the dust absorption, both internal to the source galaxy and in the lens galaxy. Second, the relation only holds for a constant star formation rate, while it seems more likely that star formation proceeded in a series of bursts. Catching the galaxy after the burst has finished, or is decreasing, implies that the UV luminosity is a strong function of age and cannot be properly related to the rate that produced these stars unless their age can be measured. All in all, the large inferred rate is better used for comparison with other galaxies, in which case this source appears to have been extremely active. Although it is more than an order of magnitude below the extremely bright SDSS J1147−0250 (Bentz et al. 2004) it is entirely consistent with the rates inferred for LBGs at $z \sim 3$ (Shapley et al. 2003) or the $\sim 40 \, M_\odot \, \text{a}^{-1}$ rate of cB58 (Pettini et al. 2002), and would explain the rapid metal enrichment of its interstellar medium sketched above.

The modeling of the lensing system (Sect. 1) also yields constraints on the effective size of the source galaxy, $\theta_{\text{eff}} = 0\rlap{.}''304$ ($2.16 \, h_{70}^{-1}$ kpc), assuming an elliptical Gaussian source[2]. Other elliptical shapes yield similar values. The compactness of the region which gives rise to this emission, combined with its tentative high metallicity may perhaps be associated with a progenitor of a present-day bulge.

Additional observations are clearly required to further constrain this lens, and to study the interstellar medium and the stellar populations at a look-back time of 88% of the present age of the universe.

---

[2] The actual shape and position angle of the source are not strongly constrained by present images.

References

Abraham, R. G., Glazebrook, K., McCarthy, P. J., et al. 2004, AJ, 127, 2455

Ando, M., Ohta, K., Iwata, I., et al. 2004, ApJ, 610, 635

Bell, E. F., Wolf, C., Meisenheimer, K., et al. 2004, ApJ, 608, 752

Bentz, M. C., Osmer, P. S., & Weinberg, D. H. 2004, ApJ, 600, L19

Blain, A. W., Frayer, D. T., Bock, J. J., & Scoville, N. Z. 2000, MNRAS, 313, 559

Bolzonella, M., Miralles, J.-M., & Pelló, R. 2000, A&A, 363, 476

Charbonneau, P. 1995, ApJS, 101, 309

Crampton, D., Schade, D., Hammer, F., et al. 2002, ApJ, 570, 86

Ellis, R., Santos, M. R., Kneib, J., & Kuijken, K. 2001, ApJ, 560, L119

Fassnacht, C. D., Moustakas, L. A., Casertano, S., et al. 2004, ApJ, 600, L155

Fosbury, R. A. E., Villar-Martín, M., Humphrey, A., et al. 2003, ApJ, 596, 797

Gebhardt, K., Faber, S. M., Koo, D. C., et al. 2003, ApJ, 597, 239

Hewitt, J. N., Turner, E. L., Lawrence, C. R., Schneider, D. P., & Brody, J. P. 1992, AJ, 104, 968

Hu, E. M., Cowie, L. L., McMahon, R. G., et al. 2002, ApJ, 568, L75

Huterer, D., Keeton, C., & Ma, C. 2004, [arXiv:astro-ph/0405040]

Jorgensen, I., Franx, M., & Kjaergaard, P. 1995, MNRAS, 273, 1097

Kassiola, A., & Kovner, I. 1993, ApJ, 417, 450

Keeton, C. R. 2001, ApJ, 561, 46

Keeton, C. R., Kochanek, C. S., & Falco, E. E. 1998, ApJ, 509, 561

Kennicutt, R. C. 1998, ARA&A, 36, 189

Kochanek, C. S., Keeton, C. R., & McLeod, B. A. 2001, ApJ, 547, 50

Koopmans, L. V. E., & Treu, T. 2002, ApJ, 568, L5

Koopmans, L. V. E., & Treu, T. 2003, ApJ, 583, 606

Kormann, R., Schneider, P., & Bartelmann, M. 1994, A&A, 284, 285

Lacy, M., Gregg, M., Becker, R. H., et al. 2002, AJ, 123, 2925

Lawrence, C. R., Schneider, D. P., Schmidet, M., et al. 1984, Science, 223, 46

McCarthy, P. J., Carlberg, R. G., Chen, H.-W., et al. 2001, ApJ, 560, L131

Miralda-Escudé, J., & Léhar, J. 1992, MNRAS, 259, 31

Pelló, R., Schaerer, D., Richard, J., Le Borgne, J.-F., & Kneib, J.-P. 2004, A&A, 416, L35

Peng, C. Y., Ho, L. C., Impey, C. D., & Rix, H. 2002, AJ, 124, 266

Pettini, M., Rix, S. A., Steidel, C. C., et al. 2002, ApJ, 569, 742

Poggianti, B. M. 1997, A&AS, 122, 399

Rusin, D., Kochanek, C. S., Falco, E. E., et al. 2003, ApJ, 587, 143

Schlegel, D. J., Finkbeiner, D. P., & Davis, M. 1998, ApJ, 500, 525

Seaton, M. J. 1979, MNRAS, 187, 73

Shapley, A. E., Erb, D. K., Pettini, M., Steidel, C. C., & Adelberger, K. L. 2004, ApJ, 612, 108

Shapley, A. E., Steidel, C. C., Pettini, M., & Adelberger, K. L. 2003, ApJ, 588, 65

Steidel, C. C., Adelberger, K. L., Shapley, A. E., et al. 2003, ApJ, 592, 728

Tonry, J. L., & Kochanek, C. S. 1999, AJ, 117, 2034

Tonry, J. L., & Kochanek, C. S. 2000, AJ, 119, 1078

Treu, T., Ellis, R. S., Liao, T. X., & van Dokkum, P. G. 2005, ApJ, 622, L5

Treu, T., & Koopmans, L. 2004, ApJ, 611, 739

Valls-Gabaud, D. 1993, ApJ, 419, 7

Warren, S. J., Hewett, P. C., Lewis, G. F., et al. 1996, MNRAS, 278, 139

Letter to the Editor